

Enantio-conversion of chiral mixtures via optical pumping

Chong Ye,^{1,2,*} Bo Liu,² Yu-Yuan Chen,² Yong Li^{2,3,†}

¹*Beijing Key Laboratory of Nanophotonics and Ultrafine Optoelectronic Systems, School of Physics, Beijing Institute of Technology, 100081 Beijing, China*

²*Beijing Computational Science Research Center, Beijing 100193, China*

³*Synergetic Innovation Center for Quantum Effects and Applications, Hunan Normal University, Changsha 410081, China*

(Dated: March 2, 2021)

Enantio-conversion with the help of electromagnetic fields is an essential issue due to the chirality-dependence of many chemical, biological, and pharmaceutical processes. Here, we propose a method for this issue based on a five-level double- Δ model of chiral molecules. By utilizing the breaking of left-right symmetry in the two Δ -type sub-structures, we can establish the chiral-state-selective excitations with one chiral ground state being excited to an achiral excited state and the other one being undisturbed. In the meanwhile, the achiral excited state will relax to the two chiral ground states. The two effects simultaneously acting on the chiral mixtures can convert molecules of different chiralities to the ones of the same chirality, i.e., the enantio-conversion via optical pumping. We numerically show that highly efficient enantio-conversion can be achieved. Our method works in the appearance of decoherences and without the precise control of pulse-durations (pulse-areas) or pulse-shapes. These advantages offer it promising features in promoting the future exploring of enantio-conversion.

I. INTRODUCTION

Recently, the inner-state enantio-purification [1–19], spatial enantio-separation [20–30], and enantio-discrimination [31–49] have become essential issues, since the vast majority of chemical [50], biological [51–53], and pharmaceutical [54–57] processes essentially depend on molecular chirality. For these purposes, the (electronic, vibrational, or rotational) inner states of chiral molecules are manipulated with the help of electromagnetic fields. Moreover, precisely manipulating the rotational populations of chiral molecules has opened new avenues to study parity violation [58, 59].

The inner-state enantio-purification includes the enantio-specific state transfer [1–12] and the enantio-conversion [13–19]. It aims to enhance the population excess of one chirality over the other in an inner state in chiral mixtures. The achieved inner-state enantiomeric excess characterizes the efficiency of the inner-state enantio-purification. The enantio-specific state transfer [1–12] achieves the enhancement of inner-state enantiomeric excess without changing the chiralities of molecules. The enantio-conversion [13–19] is more ambitious, since it aims to convert molecules of different chiralities to the ones of the same chirality.

Most proposals of the inner-state enantio-purification [1–19] are based on few-level models with left-right symmetry-breaking Δ -type (sub-) structures (e.g. the three-level Δ type model [1–13] and the four-level double- Δ model [14–19]). In these models, the chirality-dependency results from the sign difference between the products of the three electric-dipole transition

moments in the Δ -type (sub-) structures related to different chiralities. These models use only electric-dipole interactions. This property offers them advantages over the traditional chirality-dependent models usually used in enantio-discrimination [60–62], since the usually weak magnetic-dipole interactions were included in the traditional ones [60–62]. Therefore, these models are used not only in the enantio-discrimination [31–46], but also in the inner-state enantio-purification [1–19] and the spatial enantio-separation [20, 21].

Theoretical works of the inner-state enantio-purification [1–10, 13, 18, 19] based on these models focused on designing the relative phases or intensities among the electromagnetic fields for perfect (or highly efficient) inner-state enantio-purification. This purpose was achieved by using adiabatical method [1, 13], separate-pulse method [2, 3, 6, 7, 9], shortcuts-to-adiabaticity method [4], dark-state method [5, 18, 19], and Raman-pulse method [8, 10]. Recently, based on the three-level Δ -type model of chiral molecules, there were breakthrough experiments for achieving enantio-specific state transfer [11, 12] and enantio-discrimination [33–39] in gas-phase samples by manipulating the rotational states of chiral molecules with the help of electromagnetic fields.

In the experiments of enantio-specific state transfer [11, 12], only small enhancement of enantiomeric excess has been achieved. This is due to limitation factors such as the phase mismatching [43], the magnetic degeneracy [22, 43], and the thermal distributions of the rotational states [43]. The methods for solving the problems of the magnetic degeneracy [6, 63] and the thermal distributions [64] have been theoretically discussed. In addition, the decoherences as well as the requirement of the precise control of the pulse-durations (pulse-areas) [2, 3, 5–7, 9] or pulse-shapes [1, 4, 13] play an

* yechong@bit.edu.cn

† liyong@csrc.ac.cn

important limitations in achieving perfect (or highly efficient) inner-state enantio-purification.

In order to solve the problems related to the decoherences and the precise control of the pulses, we look for the possibility of using optical pumping for enantio-conversion in this paper. Optical pumping [65] is a widely used method for manipulating the inner states of quantum targets, ranging from the nuclear spin of atoms [66], quantum dot [67], hyperfine states of atoms [68] and molecules [69], to ro-vibrational (or rotational) states of molecules [70–72]. Excluding the details of different quantum targets, the key point of optical pumping is the state-selective excitations [65]. The undesired state can jump to an excited state, and the desired state cannot. This is usually attributed to the differences in the transition frequencies or transition dipoles corresponding to the undesired-excited and desired-excited transitions [65]. Simultaneously, the excited state(s) relaxes to the desired and undesired states [65]. Their combining effect will eventually convert the undesired state to the desired one [65]. In this sense, the relaxations play a positive role in manipulating the inner states and it is not necessary to precisely control the pulses in the optical pumping.

For the sake of enantio-conversion via optical pumping, the chiral-state-selective excitations are needed. Specifically, the undesired chiral state is expected to be excited to an achiral excited state(s), and in the meanwhile the desired chiral state (the inversion image of the undesired one) is expected to be undisturbed. The chiral-state-selective excitations and the relaxations act simultaneously on the chiral mixture and can eventually evoke the enantio-conversion via optical pumping: most populations will stay in the desired chiral state finally. At first glance, the chiral-state-selective excitations seem to be impossible, because a chiral state and its inversion image are degenerate by neglecting the tiny energy difference due to the fundamental weak force [59]. Further, the electric transition dipoles related to different chiralities only have possible sign-differences [1, 6, 63, 73].

We propose to realize the chiral-state-selective excitations based on a five-level double- Δ model of chiral molecules (see Fig. 1). By well designing the relative phases and intensities among the electromagnetic fields, the desired chiral ground state is an eigenstates of the system and thus is undisturbed. The undesired one is usually not an eigenstates of the system due to the breaking of left-right symmetry in the Δ -type sub-structures. It can be excited to the achiral excited state. Specifically, we use the adiabatical-elimination technology [20] to design the electromagnetic fields. Based on this, we numerically show that highly efficient enantio-conversion can be achieved via optical pumping.

II. FIVE-LEVEL DOUBLE- Δ MODEL

We consider the five-level double- Δ model of chiral molecules as shown in Fig. 1. Our working states are two degenerate (left-handed and right-handed) chiral ground states $|1_L\rangle$ and $|1_R\rangle$, two degenerate chiral mediate-energy states $|2_L\rangle$ and $|2_R\rangle$, and one achiral excited state $|3\rangle$. Here, the subscript Q ($= L, R$) denotes the chirality. The energies of the working states $|1_Q\rangle$, $|2_Q\rangle$, and $|3\rangle$ are $\hbar\omega_1$, $\hbar\omega_2$, and $\hbar\omega_3$, respectively. They are coupled via electric-dipole transitions and form two Δ -type sub-structures $|1_Q\rangle \leftrightarrow |2_Q\rangle \leftrightarrow |3\rangle \leftrightarrow |1_Q\rangle$. The frequencies of the three electromagnetic fields are ν_{21} , ν_{32} , and ν_{31} , respectively.

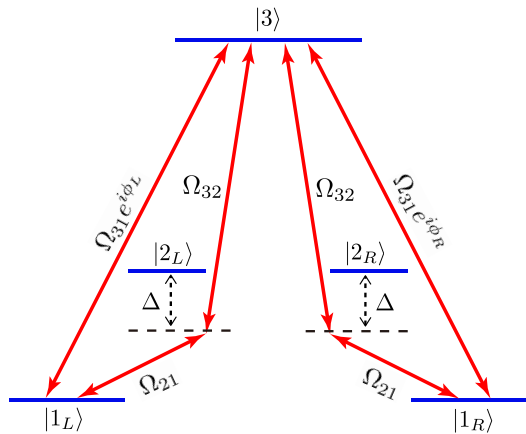


Figure 1. The five-level double- Δ model of chiral molecules. The chiral ground states $|1_Q\rangle$, the chiral mediate-energy states $|2_Q\rangle$ and the achiral excited state $|3\rangle$ are coupled with three electromagnetic fields in the Δ -type sub-structures with electric-dipole transitions $|1_Q\rangle \leftrightarrow |2_Q\rangle \leftrightarrow |3\rangle \leftrightarrow |1_Q\rangle$ in three-photon resonance condition. Here Q ($= L, R$) denotes the chirality. The corresponding coupling strengths are Ω_{21} , Ω_{32} , and $\Omega_{31}e^{i\phi_Q}$ with $\Omega_{ij} > 0$. The chirality of the two Δ -type electric-dipole sub-structures is reflected in $\phi_L = \phi$ and $\phi_R = \phi + \pi$.

We are interested in the case of the three-photon resonance. For simplicity, we assume the one-photon resonance of $|1_Q\rangle \leftrightarrow |3\rangle$. These result in

$$\Delta \equiv \Delta_{21} = -\Delta_{32}, \quad \Delta_{31} = 0. \quad (1)$$

The detunings are $\Delta_{ij} \equiv \omega_i - \omega_j - \nu_{ij}$ with $i, j = 1, 2, 3$ and $i > j$. By using the rotating-wave approximation, the five-level double- Δ model can be described by the Hamiltonian in the interaction picture ($\hbar = 1$)

$$\hat{H} = \sum_Q [\Delta |2_Q\rangle\langle 2_Q| + (\Omega_{21}|1_Q\rangle\langle 2_Q| + \Omega_{32}|2_Q\rangle\langle 3| + \Omega_{31}e^{i\phi_Q}|1_Q\rangle\langle 3| + \text{H.c.})]. \quad (2)$$

The chirality is reflected in the overall phases [14, 16, 17]

$$\phi_L \equiv \phi, \quad \phi_R = \phi + \pi. \quad (3)$$

For the sake of simplicity and without loss of generality, we have assumed that all $\Omega_{ij} > 0$.

In the following, we will discuss the physical realization of the five-level double- Δ model. In the gas-phase experiments of enantio-discrimination [33–39] and the enantio-specific state transfer [11, 12], the rotational sub-levels are introduced [6, 11, 12, 22, 33–39, 63] in order to consider the molecular rotations. We focus on the case of chiral asymmetric-top molecules. For these chiral molecules, when the rotational sub-levels of the working states as well as the polarizations and the frequencies of the three electromagnetic fields are well designed, the involvement of rotational sub-levels will not challenge the few-level models [6, 63]. Specifically, we can choose the rotational sub-levels of $|1_Q\rangle$, $|2_Q\rangle$, $|3\rangle$ to be $|J_{k_a k_c M} = 0_{000}\rangle$, $|1_{010}\rangle$, and $(|1_{101}\rangle + |1_{10-1}\rangle)/\sqrt{2}$ [6, 63], respectively. $|J_{k_a k_c M}\rangle$ are the eigenstates of asymmetric-top molecules [6, 63]. The three electromagnetic fields coupling with the electric-dipole transitions $|1_Q\rangle \leftrightarrow |2_Q\rangle \leftrightarrow |3\rangle \leftrightarrow |1_Q\rangle$ are Z -, X -, and Y -polarized in the space-fixed frame, respectively.

Here, we will specify the vibrational sub-levels of the working states. The chirality of molecules is related to the double-well-type energy surface potential in a vibrational degree of freedom. One chiral state and its degenerate inversion image are localized in the two wells, respectively. They are not the eigenstates of the double-well potential. The tunneling between them would make the enantio-purified molecules change to the opposite chirality and thus would reduce the achieved enantiomeric excess. For some chiral molecules, the effect of tunneling is sufficient weak [74] or can be suppressed due to the environments [75–86]. In our discussions, we have assumed that the tunneling between degenerate chiral states of different chiralities are negligible [18]. Further, the couplings among electronic, vibrational, and rotational degrees of freedom will introduce effective couplings among our work states and other states. Then, the molecules will leak out of the working model, and the few-level model may become insufficient to describe the dynamics of the chiral molecules. Here, we have assumed that these couplings are negligible in the framework of Born-Oppenheimer approximation [6, 18]. These two assumptions will play as main limitations putting on target molecules by using our method of enantio-conversion.

Upon these assumptions and approximations, the vibrational sub-levels of $|1_L\rangle$ and $|2_L\rangle$ can be chosen as the vibrational ground state in one well of the double-well potential, since the their rotational sub-levels are different. Its inversion image gives the vibrational sub-levels of $|1_R\rangle$ and $|2_R\rangle$. We note that the vibrational sub-levels of chiral states $|1_L\rangle$ and $|2_L\rangle$ can also be chosen as the vibrational ground and higher-energy states in one well of the double-well potential, respectively. The vibrational sub-level of the achiral state $|3\rangle$ can be a vibrational excited state near or beyond the barrier of the double-well potential.

For gas-phase molecules [11, 12, 33–39], the propaga-

tion directions of the three electromagnetic fields can not be parallel due to the special requirement in their polarizations [6, 63] (e.g. as in our discussions, the polarization directions are mutually vertical to each other). This gives rise to the phase-mismatching problem [11, 12, 33–39]. However, when the typical length of the molecule-field interaction volume is much smaller than the largest wavelength among those of the three electromagnetic fields, the molecules are approximately phase-matched. Therefore, throughout our discussions we assume that the molecules are phase matched and described by the same Hamiltonian.

III. CHIRAL-STATE-SELECTIVE EXCITATIONS

For chiral molecules, we will utilize the difference between the overall phases ϕ_L and ϕ_R to establish the required chiral-state-selective excitations. Although the relaxations are indispensable and important in optical pumping, in order to highlight the physical mechanism of our chiral-state-selective excitations, we will not consider the relaxations during evolution in this section.

In the large-detuning region with $|\Delta| \gg \Omega_{32} \sim \Omega_{21} \gg \Omega_{31}$, we use the Fröhlich-Nakajima transformation [87, 88] of $\exp(\hat{S})$ for the Hamiltonian (2). The anti-Hermitian operator is

$$\hat{S} = \frac{1}{\Delta} \sum_Q (\Omega_{21}|1_Q\rangle\langle 2_Q| + \Omega_{32}|3\rangle\langle 2_Q| - \text{H.c.}), \quad (4)$$

which satisfies $[\hat{H}_0, \hat{S}] + \hat{H}_1 = 0$. The zero-order, first-order, and second-order Hamiltonian are $\hat{H}_0 = \sum_Q \Delta|2_Q\rangle\langle 2_Q|$, $\hat{H}_1 = \sum_Q (\Omega_{21}|1_Q\rangle\langle 2_Q| + \Omega_{32}|2_Q\rangle\langle 3| + \text{H.c.})$, and $\hat{H}_2 = \sum_Q (\Omega_{31}e^{i\phi_Q}|1_Q\rangle\langle 3| + \text{H.c.})$, respectively. The transformed Hamiltonian is

$$\begin{aligned} \hat{H}' &= \exp(-\hat{S})\hat{H}\exp(\hat{S}) \simeq \hat{H}_0 + [\hat{H}_1, \hat{S}]/2 + \hat{H}_2 \\ &= \sum_Q \tilde{\Delta}|2_Q\rangle\langle 2_Q| + (\Lambda|2_L\rangle\langle 2_R| + \text{H.c.}) + 2\Lambda|3\rangle\langle 3| \\ &\quad + \sum_Q [\tilde{\Lambda}|1_Q\rangle\langle 1_Q| + (\tilde{\Omega}_Q|1_Q\rangle\langle 3| + \text{H.c.})]. \end{aligned} \quad (5)$$

Here, we have defined $\Lambda \equiv -\Omega_{32}^2/\Delta$, $\tilde{\Lambda} \equiv -\Omega_{21}^2/\Delta$, $\tilde{\Delta} \equiv \Delta - \Lambda - \tilde{\Lambda}$, and

$$\tilde{\Omega}_Q \equiv \Omega_{31}e^{i\phi_Q} - \frac{\Omega_{32}\Omega_{21}}{\Delta}. \quad (6)$$

From Eq. (5), we can see that the evolution of the initial chiral ground states $|1_Q\rangle$ will not be affected by the chiral mediate-energy states $|2_Q\rangle$. Thus, the chiral mediate-energy states $|2_Q\rangle$ can be adiabatically eliminated. This process gives the following reduced three-level Hamiltonian

$$\hat{\mathcal{H}} = 2\Lambda|3\rangle\langle 3| + \sum_Q [\tilde{\Lambda}|1_Q\rangle\langle 1_Q| + (\tilde{\Omega}_Q|1_Q\rangle\langle 3| + \text{H.c.})]. \quad (7)$$

By further tuning the three electromagnetic fields to ensure

$$\phi = 0, \quad \Omega_{31} = \frac{\Omega_{32}\Omega_{21}}{\Delta}, \quad (8)$$

i.e., $\tilde{\Omega}_L = 0$ and $\tilde{\Omega}_R = -2\Omega_{31}$, we can arrive the Hamiltonian

$$\hat{\mathcal{H}}_{\text{eff}} = 2\Lambda|3\rangle\langle 3| - 2\Omega_{31}(|1_R\rangle\langle 3| + \text{H.c.}) + \sum_Q \tilde{\Lambda}|1_Q\rangle\langle 1_Q|. \quad (9)$$

The left-handed ground state $|1_L\rangle$ is an eigenstate of the effective Hamiltonian (9). The right-handed ground state $|1_R\rangle$ is coupled to $|3\rangle$ in the effective Hamiltonian (9). Therefore, we expect that $|1_L\rangle$ will be undisturbed by the electromagnetic fields, and $|1_R\rangle$ will be excited, i.e., achieving the chiral-state-selective excitations.

The mediate-energy states $|2_L\rangle$ and $|2_R\rangle$ are important in establishing the chiral-state-selective excitations. They are introduced to establish the two-photon processes $|1_Q\rangle \leftrightarrow |2_Q\rangle \leftrightarrow |3\rangle$. The chirality-dependent interferences between the two-photon processes and the one-photon processes $|1_Q\rangle \leftrightarrow |3\rangle$ can give rise to the chirality-dependent dynamics for the two enantiomers. In the large-detuning region, we have adiabatically eliminated the mediate-energy states in the large-detuning region to yield the effective coupling of $\Omega_{32}\Omega_{21}/\Delta$ [i.e., the second term in Eq. (6)]. The effective Hamiltonian (7) clearly shows the chirality-dependent interferences. By further tuning the electromagnetic fields, we can establish the chiral-state-selective excitations as indicated by Hamiltonian (9).

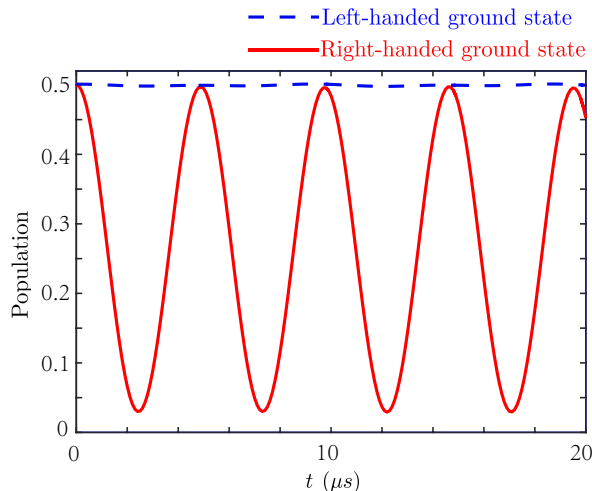


Figure 2. Chiral-state-selective excitations: evolution of populations in the left-handed and right-handed ground states. The initial state is $\rho(t=0) = \sum_Q |1_Q\rangle\langle 1_Q|/2$. The parameters are $\phi = 0$, $\Delta = 2\pi \times 20$ MHz, $\Omega_{21} = 2\pi \times 1$ MHz, $\Omega_{32} = 2\pi \times 1$ MHz and $\Omega_{31} = 2\pi \times 0.05$ MHz.

In Fig. 2, we demonstrate the expected chiral-state-selective excitations by numerically solving $\dot{\rho} = -i[\hat{H}, \rho]$

for an initial racemic mixture with each molecule described by $\rho(t=0) = \sum_Q |1_Q\rangle\langle 1_Q|/2$. We take the typical experimental available parameters [6, 18]: $\Delta = 2\pi \times 20$ MHz, $\Omega_{32} = \Omega_{21} = 2\pi \times 1$ MHz, $\Omega_{31} = 2\pi \times 0.05$ MHz, and $\phi = 0$ (more discussions about these parameters are shown in Appendix). The numerical results clearly show that only the right-handed ground state $|1_R\rangle$ is excited and the left-handed ground state $|1_L\rangle$ approximately remains unchanged.

We note that when the overall phase $\phi = 0$ changes to be $\phi = \pi$, the dynamics of the two chiral ground states exchange to each other [5, 18, 44]. Then, with the same process as above, the right-handed ground state $|1_R\rangle$ will be undisturbed by the electromagnetic fields and the left-handed ground state $|1_L\rangle$ will be excited. For convenience, we will only focus on the cases with $\phi = 0$ in the following discussions.

IV. ENANTIO-CONVERSION VIA OPTICAL PUMPING

Now, we have established the chiral-state-selective excitations without the consideration of the relaxations. The relaxations are ineluctable in the realistic cases [11, 12, 33–39], and important for the realization of our method. In the following, we will show that when the electromagnetic fields are well designed as in Sec. III, the combining effect of the relaxations and the chiral-state-selective excitations can give rise to the enantio-conversion via optical pumping. Now the evolution of the density operator ρ obeys the master equation

$$\frac{d\rho}{dt} = -i[\hat{H}, \rho] + \mathcal{L}\rho. \quad (10)$$

The effect of decoherences are described by the super-operator $\mathcal{L}\rho$. It can be divided into $\mathcal{L}\rho = \mathcal{L}_{r1}\rho + \mathcal{L}_{dp}\rho$. The term of pure population relaxation $\mathcal{L}_{r1}\rho$ reads

$$\begin{aligned} \mathcal{L}_{r1}\rho = & \sum_Q [\gamma_{21}(\hat{\sigma}_{1_Q 2_Q} \rho \hat{\sigma}_{2_Q 1_Q} - \hat{\sigma}_{2_Q 1_Q} \rho \hat{\sigma}_{1_Q 2_Q}) \\ & + \sum_{n=1}^2 \gamma_{3n}(\hat{\sigma}_{n_Q 3} \rho \hat{\sigma}_{3 n_Q} - \hat{\sigma}_{n_Q 3} \rho \hat{\sigma}_{3 n_Q})] + \text{H.c.} \end{aligned} \quad (11)$$

with chirality-independent [17] relaxation rates γ_{3n} and γ_{21} . We have defined that $\hat{\sigma}_{pq} \equiv |p\rangle\langle q|$ ($p, q = 1_Q, 2_Q, 3$). We have also considered the effect of pure dephasings, which is also ineluctable in the realistic cases [11, 12, 33–39]. The term of pure dephasing reads [89]

$$\mathcal{L}_{dp}\rho = -\tilde{\gamma} \sum_{p,q} \hat{\sigma}_{pp} \rho \hat{\sigma}_{qq}, \quad (p \neq q). \quad (12)$$

It only causes the decrease of off-diagonal terms of ρ . We have assumed that the pure dephasing rate $\tilde{\gamma}$ is state-independent for the sake of simplicity [90].

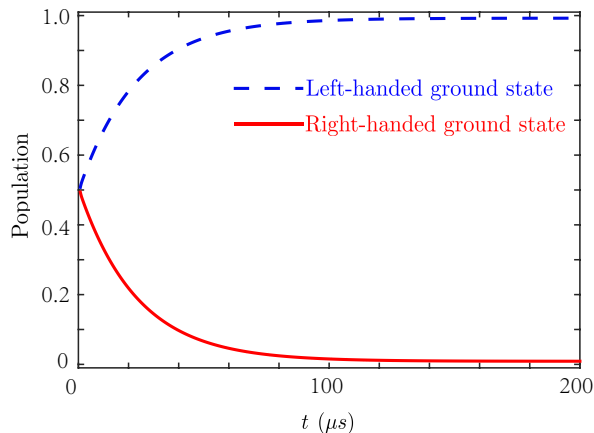


Figure 3. Optical pumping method of enantio-conversion: evolution of populations in the left-handed and right-handed ground states. The initial state is $\rho(t=0) = \sum_Q |1_Q\rangle\langle 1_Q|/2$. We choose the decoherence rates as $\gamma_{31} = \gamma_{32} = 2\pi \times 0.1$ MHz and $\gamma_{21} = \tilde{\gamma} = 2\pi \times 1$ MHz. The parameters are $\phi = 0$, $\Delta = 2\pi \times 20$ MHz, $\Omega_{21} = 2\pi \times 1$ MHz, $\Omega_{32} = 2\pi \times 1$ MHz, and $\Omega_{31} = 2\pi \times 0.05$ MHz.

Specifically, we choose the typical decoherence rates in gas-phase experiments [11, 12, 33–39]: $\gamma_{31} = \gamma_{32} = 2\pi \times 0.1$ MHz and $\gamma_{21} = \tilde{\gamma} = 2\pi \times 1$ MHz (more discussions are shown in Appendix). The results by numerically solving master equations (10) are shown in Fig. 3. They clearly show that the dynamics of the system are intensely changed by the decoherences. The combining effect of the chiral-state-selective excitations and the decoherences results in the conversion of molecules from $|1_L\rangle$ to $|1_R\rangle$. We are interested in the enantiomeric excess in the chiral ground states defined as

$$\varepsilon \equiv \frac{|\langle 1_L|\rho|1_L\rangle - \langle 1_R|\rho|1_R\rangle|}{|\langle 1_L|\rho|1_L\rangle + \langle 1_R|\rho|1_R\rangle|}. \quad (13)$$

The achieved enantiomeric excess ($t \geq 140 \mu s$) in Fig. 3 is $\varepsilon = 99.2\%$, i.e., highly efficient enantio-conversion is achieved.

A. Role of relaxations and dephasings

Now, we have shown the possibility of highly efficient enantio-conversions by optical pumping. When the chiral-state-selective excitations and the relaxations act simultaneously on the chiral mixture, the system gradually reaches its steady state and finally most molecules are transferred to that of the same chirality. Here, we would like to discuss how the enantio-conversion depends on relaxation and dephasing rates. For this purpose, we explore the steady states of the system related to the master equation (10). Specifically, we solve the equations $-i[\hat{H}, \rho] + \mathcal{L}\rho = 0$.

For simplicity, we choose $\gamma_{31} = \gamma_{32} = \gamma_{21} = \gamma$. In Fig. 4(a), we show how the achieved enantiomeric ex-

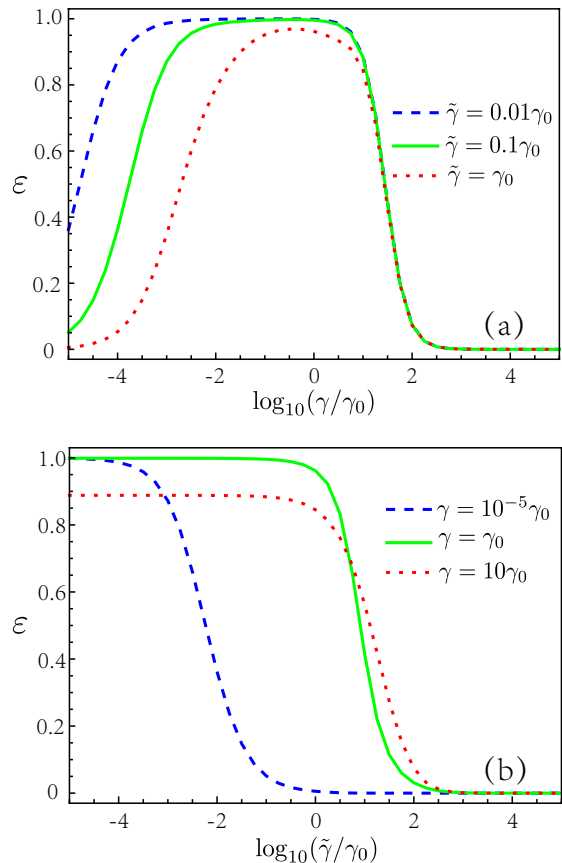


Figure 4. Achieved enantiomeric excess ε in the steady states. $\gamma_0 = 2\pi \times 1$ MHz. The parameters are $\phi = 0$, $\Delta = 2\pi \times 20$ MHz, $\Omega_{21} = 2\pi \times 1$ MHz, $\Omega_{32} = 2\pi \times 1$ MHz and $\Omega_{31} = 2\pi \times 0.05$ MHz. (a) ε as a function of γ ($= \gamma_{31} = \gamma_{32} = \gamma_{21}$) for different dephasing rates $\tilde{\gamma}$. (b) ε as a function of $\tilde{\gamma}$ for different relaxation rates γ ($= \gamma_{31} = \gamma_{32} = \gamma_{21}$).

cess ε (in the steady state) varies with the relaxation rate γ for different dephasing rates $\tilde{\gamma}$. Specifically, we would like to take the case of $\tilde{\gamma} = 0.01\gamma_0$ (the blue dashed line) as an example. When γ is very small (e.g. $\gamma < 10^{-3}\gamma_0$), the achieved enantiomeric excess ε is not high. In that region, the achieved enantiomeric excess ε increases with γ . In the large relaxation region (e.g. $\gamma > 10\gamma_0$), the achieved enantiomeric excess will decrease with γ . Then, the highly efficient enantio-conversions can only be achieved in a mediated region of γ .

These phenomena indicate that the relaxations play a complicate role in optical pumping for enantio-conversion. The relaxations make the achiral excited molecules, which was transferred from the undesired chiral ground state due to the chiral-state-selective excitations, relax to the desired chiral ground state. In this sense, the relaxations are indispensable. However, the relaxations should not be very strong, since they may destroy the chiral-state-selective excitations.

Further, we compare the results for different dephasing rates in Fig. 4(a). For the case of small dephasing

rate $\tilde{\gamma} = 0.01\gamma_0$ (the blue dashed line), highly efficient enantio-conversions (e.g. $\varepsilon \geq 99\%$) can be achieved in a wide region. Here, we have used $\gamma_0 = 2\pi \times 1$ MHz. For the case of larger dephasing rate $\tilde{\gamma} = 0.1\gamma_0$ (the green solid line), highly efficient enantio-conversions can be achieved in a narrower region. By further increasing the dephasing rate to $\tilde{\gamma} = \gamma_0$ (the blue dashed line), highly efficient enantio-conversions cannot be achieved.

In order to explore the role of the dephasings, we show how the achieved enantiomeric excess ε varies with $\tilde{\gamma}$ for different relaxation rates γ ($= \gamma_{31} = \gamma_{32} = \gamma_{21}$) in Fig. 4 (b). It is shown that the achieved enantiomeric excess will decrease with the increase of the dephasing rates $\tilde{\gamma}$.

B. Highly efficient enantio-conversion in strong relaxation region

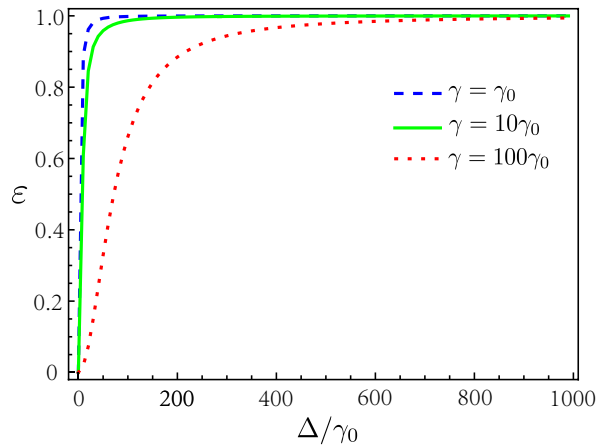


Figure 5. Achieved enantiomeric excess in the steady states as a function of Δ for different γ ($= \gamma_{21} = \gamma_{32} = \gamma_{31}$). Other parameters are chosen as $\tilde{\gamma} = 2\pi \times 1$ MHz, $\Omega_{21} = 2\pi \times 1$ MHz, and $\Omega_{32} = 2\pi \times 1$ MHz. The coupling strength Ω_{32} is adjusted correspondingly to ensure $\Omega_{31} = \Omega_{32}\Omega_{21}/\Delta$. We use $\gamma_0 = 2\pi \times 1$ MHz.

We have shown that the relaxations are indispensable for enantio-conversion via optical pumping, but should be not too strong to destroy the chiral-state-selective excitations. Here, we would like to discuss the possibility of achieving highly efficient enantio-conversion in the strong relaxation region.

For this purpose, we increase the detuning Δ and simultaneously decrease the coupling strength Ω_{31} to ensure $\Omega_{31} = \Omega_{32}\Omega_{21}/\Delta$. In Fig. 5, we show the achieved enantiomeric excess as a function of Δ for different γ ($= \gamma_{21} = \gamma_{32} = \gamma_{31}$). Other parameters are chosen as $\tilde{\gamma} = 2\pi \times 1$ MHz, $\phi = 0$, $\Omega_{21} = 2\pi \times 1$ MHz and $\Omega_{32} = 2\pi \times 1$ MHz. The numerical results show that highly efficient enantio-conversion can be achieved in the strong relaxation region. **These results can be understood as follows. In the large-detuning region with $|\Delta| \gg \Omega_{32} \sim \Omega_{21} \gg \Omega_{31}$, the three-level Hamiltonian (7) can be used to approximately replace the system's orig-**

inal Hamiltonian (2). By further adjusting the fields, we achieve the chiral-state-selective excitation as shown in the system's approximate Hamiltonian (9). The larger the detuning Δ is (or the smaller coupling strengths are), the more robust the approximation is. When a system's Hamiltonian is exactly described by Eq. (9), the undesired chiral ground state can be perfectly transferred to the desired chiral ground state by optical pumping in the steady state. In this sense, the larger detuning Δ is (or the smaller coupling strengths are), the higher achieved enantiomeric excess is.

C. Effect of relaxations out of the five-level model

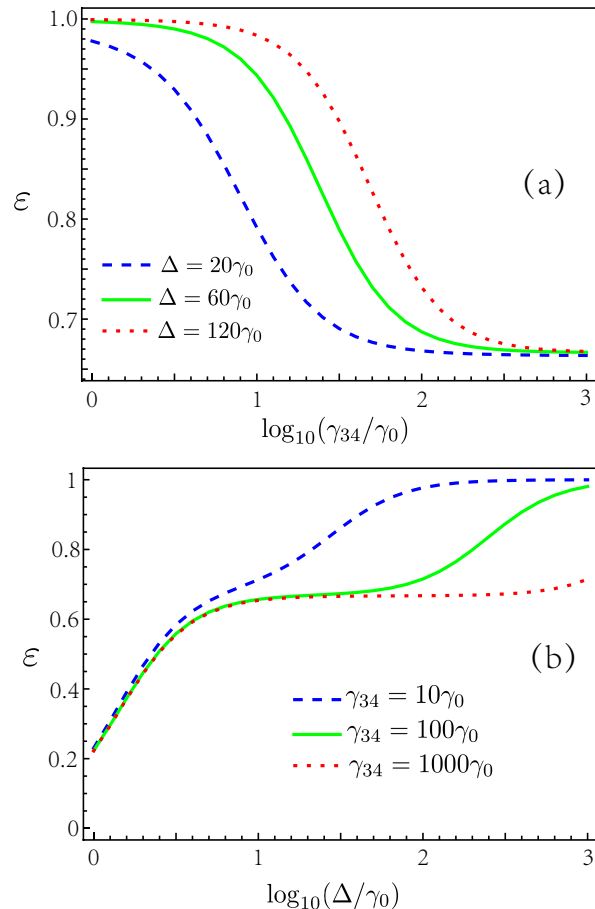


Figure 6. Achieved enantiomeric excess in steady states as a function of (a) γ_{34} and (b) Δ . The coupling strengths are simultaneously adjusted to ensure $\Omega_{31} = \Omega_{32}\Omega_{21}/\Delta$ in the appearance of relaxation out of the five-level model. Other parameters are $\gamma_{41} = 2\pi \times 10^{-5}$ MHz, $\gamma_{31} = \gamma_{32} = 2\pi \times 0.1$ MHz, $\gamma_{21} = \tilde{\gamma} = 2\pi \times 1$ MHz, $\phi = 0$, and $\Omega_{21} = \Omega_{32} = 2\pi \times 1$ MHz. We use $\gamma_0 = 2\pi \times 1$ MHz.

So far, we have assumed that the excited molecules will not relax out of the five-level model in our calculations and discussions. In the realistic case, the molecules in the achiral excited state can relax to the lower-energy chiral

states out of the five-level model [91]. The relaxation rates from these chiral states to their corresponding chiral ground states may be very small [91]. Here, we would like to explore the effect of such a process on the optical pumping for enantio-conversion.

To this end, we introduce additional chiral states $|4_L\rangle$ and $|4_R\rangle$. We describe the relaxation and the dephasing related to them in the same manner as Eq. (11) and Eq. (12), respectively. For relaxations from $|4_Q\rangle$ to $|1_Q\rangle$ ($Q = L, R$), we choose a very small relaxation rate $\gamma_{41} = 2\pi \times 10^{-5}$ MHz. The relaxation rates from the achiral excited state $|3\rangle$ to $|4_Q\rangle$ is describe by γ_{34} .

In Fig. 6(a), we show the achieved enantiomeric excess in the steady states as a function of γ_{34} for different detuning Δ . We find that the achieved enantiomeric excess ε decreases with the increase of the relaxation rate γ_{34} and approaches to a constant value ($\sim 60\%$). Comparing the results for different detunings, we find that the achieved enantiomeric excess can be improved by increasing the detuning Δ . In Fig. 6(b), we show how the increase of the detuning Δ can increase the achieved enantiomeric excess. In Fig. 6, the coupling strengths are simultaneously adjusted to ensure $\Omega_{31} = \Omega_{32}\Omega_{21}/\Delta$. Other parameters are $\gamma_{31} = \gamma_{32} = 2\pi \times 0.1$ MHz, $\gamma_{21} = 2\pi \times 1$ MHz, $\phi = 0$, and $\Omega_{21} = \Omega_{32} = \tilde{\gamma} = 2\pi \times 1$ MHz.

V. SUMMARY

We have used the five-level double- Δ model of chiral molecules to demonstrate that the highly efficient enantio-conversion can be achieved when the system reaches its steady state via optical pumping. The chiral-state-selective excitations can be generated by well designing the relative phases and intensities among the three electromagnetic fields with the help of the adiabatical elimination technology. The relaxations among our working states are indispensable in our method. When the relaxations and the chiral-state-selective excitations simultaneously act on the chiral mixture, the highly efficient enantio-conversion can be achieved. However, the relaxations should not be too strong to destroy the chiral-state-selective excitations. We also find that the efficiency of the enantio-conversion will decrease with the increase of the dephasing rates. In addition, the relaxation out of the working states can also reduce the efficiency of the enantio-conversion via optical pumping. Fortunately, our numerical results have shown that these negative effects can be weakened by increasing the detunings Δ and simultaneously reducing the coupling strength Ω_{31} to ensure $\Omega_{31} = \Omega_{32}\Omega_{21}/\Delta$. In addition, in the whole process of optical pumping, the relative phases and strengths of the three electromagnetic fields should be well controlled.

One key point of our optical pumping method for enantio-conversions is using the left-right symmetry-breaking in Δ -type (sub-)structures to establish the chiral-state-selective excitations. The other key point is the relaxations from the achiral excited state to the chi-

ral ground states. In our five-level double- Δ model with one achiral excited state, we have appropriately chosen the applied electromagnetic fields in the large-detuning condition such that the original model can be reduced to a three-level model. In the reduced three-level model with one achiral excited state, the achiral excited state is coupled with the two chiral ground states on-resonance. By further adjusting the applied electromagnetic fields, the coupling strength corresponding to one chiral ground state can be zero and simultaneously that corresponding to the other one is nonzero, i.e, achieving the chiral-state-selective excitations. When the chiral-state-selective excitations and the relaxations act simultaneously on the chiral mixture, the enantio-conversion via optical pumping can be achieved. In this sense, the four-level double- Δ model [14–19] can also be used to realise enantio-conversions via optical pumping, since it have chirality-dependent Δ -type (sub-)structures and achiral excited states. In Ref. [18], it was shown that the four-level double- Δ model [14–19] can be simplified to two uncoupled two-level subsystems by appropriately choosing the applied fields. The two uncoupled two-level subsystems have the same coupling strengths but different detunings [18]. By further adjusting the applied fields, one subsystem will be on-resonance and the other one will be in large-detuning limit. Then, one chiral ground state will be excited and the other will be undisturbed, i.e., achieving the chiral-state-selective excitations. Similar as the case of the five-level model, the chiral-state-selective excitations and the relaxations act simultaneously on the chiral mixture and can eventually evoke the enantio-conversion via optical pumping in the four-level double- Δ model [14–19].

ACKNOWLEDGEMENT

This work was supported by the National Key R&D Program of China grant (2016YFA0301200), the Natural Science Foundation of China (under Grants No. 11774024, No. 12074030, No. U1930402 and No. 11947206), and the Science Challenge Project (under Grant No. TZ2018003).

Appendix: Typical parameters for gas-phase chiral molecules

Here, we give typical parameters for gas-phase chiral molecules according to the gas-phase experiments of the enantio-discrimination [33–39] and the enantio-specific state transfer [11, 12]. In our method, the transitions $|3\rangle \leftrightarrow |1_Q\rangle$ and $|3\rangle \leftrightarrow |2_Q\rangle$ are ro-vibrational transitions. The transitions $|2_Q\rangle \leftrightarrow |1_Q\rangle$ can be purely rotational transitions or ro-vibrational transitions. Typical experimentally available coupling strengths for rotational transitions of chiral molecules are about $2\pi \times 10$ MHz

or less [11, 12, 33–39]. Usually, the electric-dipole moments of ro-vibrational transitions are much smaller than that of purely rotational transitions. Since the intensity of an infrared electromagnetic field can be easily made much larger than that of microwave ones, the coupling strengths of ro-vibrational transitions can have the same magnitude as that of purely rotational transitions [6].

In our calculations, the coupling strengths ($\leq 2\pi \times 1$ MHz) are chosen to be much smaller than the experimental available ones ($2\pi \times 10$ MHz). The reason is as follows. When the electromagnetic fields are applied to manipulate the chiral molecules, the sample can also be heated. This will prevent the realization of our method as well as the enantio-discrimination [33–39] and the enantio-specific state transfer [11, 12]. The detunings in our calculations are $\Delta_{21} = -\Delta_{32} = \Delta = 2\pi \times 20$ MHz and $\Delta_{13} = 0$. The detunings and coupling strengths are much smaller than the typical ro-vibrational and rotational transition frequencies of chiral molecules. Then, the rotating-wave approximation can be used in our model [18] and the effect of other selection-rule-allowed

transitions of chiral molecules on our model is negligible [18].

The parameters of decoherences are chosen as follows. The decoherence mechanisms of chiral molecules in gas-phase are spontaneous emission and collision. For rotational transitions, the collision dominates and gives the typical rotational relaxation and dephasing rates of about $2\pi \times 1$ MHz [11, 12, 33–39]. Since the dephasing varies modestly with molecule, vibrational state, and rotational state [90], we have chosen the state-independent dephasing rate $\tilde{\gamma} = 2\pi \times 1$ MHz. Due to the large transition frequencies, the typical ro-vibrational relaxation rates due to collision are much smaller than the rotational relaxation rates [90]. For ro-vibrational transitions, the relaxations due to spontaneous emission becomes a possible relaxation mechanism, in addition to collisions with other molecules [6]. Therefore, we have chosen the relaxation rate for ro-vibrational transitions as about $2\pi \times 0.1$ MHz. Specifically, we have chosen $\gamma_{31} = \gamma_{32} = 2\pi \times 0.1$ MHz corresponding to the two ro-vibrational transitions. Since the transitions $|1_Q\rangle \leftrightarrow |2_Q\rangle$ can be purely rotational, we have chosen $\gamma_{21} = 2\pi \times 1$ MHz.

-
- [1] P. Král and M. Shapiro, Phys. Rev. Lett. **87**, 183002 (2001).
- [2] Y. Li and C. Bruder, Phys. Rev. A **77**, 015403 (2008).
- [3] W. Z. Jia and L. F. Wei, J. Phys. B: At. Mol. Opt. Phys. **43**, 185402 (2010).
- [4] N. V. Vitanov and M. Drewsen, Phys. Rev. Lett. **122**, 173202 (2019).
- [5] C. Ye, Q. Zhang, Y.-Y. Chen, and Y. Li, Phys. Rev. A **100**, 043403 (2019).
- [6] M. Leibscher, T. F. Giesen, and C. P. Koch, J. Chem. Phys. **151**, 014302 (2019).
- [7] J.-L. Wu, Y. Wang, J. Song, Y. Xia, S.-L. Su, and Y.-Y. Jiang, Phys. Rev. A **100**, 043413 (2019).
- [8] J.-L. Wu, Y. Wang, J.-X. Han, C. Wang, S.-L. Su, Y. Xia, Y.-Y. Jiang, and J. Song, Phys. Rev. Applied **13**, 044021 (2020).
- [9] B. T. Torosov, M. Drewsen, and N. V. Vitanov, Phys. Rev. A **101**, 063401 (2020).
- [10] B. T. Torosov, M. Drewsen, and N. V. Vitanov, Phys. Rev. Research **2**, 043235 (2020).
- [11] S. Eibenberger, J. Doyle, and D. Patterson, Phys. Rev. Lett. **118**, 123002 (2017).
- [12] C. Pérez, A. L. Steber, S. R. Domingos, A. Krin, D. Schmitz, and M. Schnell, Angew. Chem. Int. Ed. **56**, 12512 (2017).
- [13] P. Král, I. Thanopoulos, M. Shapiro, and D. Cohen, Phys. Rev. Lett. **90**, 033001 (2003).
- [14] M. Shapiro, E. Frishman, and P. Brumer, Phys. Rev. Lett. **84**, 1669 (2000).
- [15] P. Brumer, E. Frishman, and M. Shapiro, Phys. Rev. A **65**, 015401 (2001).
- [16] D. Gerbasi, M. Shapiro, and P. Brumer, J. Chem. Phys. **115**, 5349 (2001).
- [17] E. Frishman, M. Shapiro, and P. Brumer, J. Phys. B: At. Mol. Opt. Phys. **37** 2811 (2004).
- [18] C. Ye, Q. Zhang, Y.-Y. Chen, and Y. Li, Phys. Rev. Research, **2**, 033064 (2020).
- [19] C. Ye, Q. Zhang, Y.-Y. Chen, and Y. Li, arXiv: 2001.07834 (2020).
- [20] Y. Li, C. Bruder, and C. P. Sun, Phys. Rev. Lett. **99**, 130403 (2007).
- [21] X. Li and M. Shapiro, J. Chem. Phys. **132**, 194315 (2010).
- [22] A. Jacob and K. Hornberger, J. Chem. Phys. **137**, 044313 (2012).
- [23] A. Eilam and M. Shapiro, Phys. Rev. Lett. **110**, 213004 (2013).
- [24] R. P. Cameron, S. M. Barnett, and A. M. Yao, New J. Phys. **16**, 013020 (2014).
- [25] D. S. Bradshaw and D. L. Andrews, New J. Phys. **16** 103021 (2014).
- [26] D. S. Bradshaw and D. L. Andrews, Opt. Lett. **40**, 000677 (2015).
- [27] P. Barcellona, R. Passante, L. Rizzuto, and S. Y. Buhmann, Phys. Rev. A **93**, 032508 (2016).
- [28] P. Barcellona, H. Safari, A. Salam, and S. Y. Buhmann, Phys. Rev. Lett. **118**, 193401 (2017).
- [29] C. Brand, B. A. Stickler, C. Knobloch, A. Shayeghi, K. Hornberger, and M. Arndt, Phys. Rev. Lett. **121**, 173002 (2018).
- [30] N. Kravets, A. Aleksanyan, and E. Brasselet, Phys. Rev. Lett. **122**, 024301 (2019).
- [31] W. Z. Jia and L. F. Wei, Phys. Rev. A **84**, 053849 (2011).
- [32] E. Hirota, Proc. Jpn. Acad. Ser. B **88**, 120 (2012).
- [33] D. Patterson, M. Schnell, and J. M. Doyle, Nature (London) **497**, 475 (2013).
- [34] D. Patterson and J. M. Doyle, Phys. Rev. Lett. **111**, 023008 (2013).
- [35] D. Patterson and M. Schnell, Phys. Chem. Chem. Phys. **16**, 11114 (2014).

- [36] V. A. Shubert, D. Schmitz, D. Patterson, J. M. Doyle, and M. Schnell, *Angew. Chem. Int. Ed.* **53**, 1152 (2014).
- [37] V. A. Shubert, D. Schmitz, C. Medcraft, A. Krin, D. Patterson, J. M. Doyle, and M. Schnell, *J. Chem. Phys.* **142**, 214201 (2015).
- [38] S. Lobsiger, C. Pérez, L. Evangelisti, K. K. Lehmann, and B. H. Pate, *J. Phys. Chem. Lett.* **6**, 196 (2015).
- [39] V. A. Shubert, D. Schmitz, C. Pérez, C. Medcraft, A. Krin, S. R. Domingos, D. Patterson, and M. Schnell, *J. Phys. Chem. Lett.* **7**, 341 (2015).
- [40] K. K. Lehmann, arXiv: 1501.05282 (2015); 1501.07874 (2015).
- [41] A. Yachmenev and S. N. Yurchenko, *Phys. Rev. Lett.* **117**, 033001 (2016).
- [42] K. K. Lehmann, in *Frontiers and Advances in Molecular Spectroscopy*, edited by J. Laane (Elsevier, 2018), Vol. 2, pp. 713-743.
- [43] K. K. Lehmann, *J. Chem. Phys.* **149**, 094201 (2018).
- [44] C. Ye, Q. Zhang, Y.-Y. Chen, and Y. Li, *Phys. Rev. A* **100**, 033411 (2019).
- [45] Y.-Y. Chen, C. Ye, Q. Zhang, and Y. Li, *J. Chem. Phys.* **152**, 204305 (2020).
- [46] X.-W. Xu, C. Ye, Y. Li, and A.-X. Chen, *Phys. Rev. A* **102**, 033727 (2020).
- [47] K. A. Forbes and D. L. Andrews, *Opt. Lett.* **43**, 000435 (2018).
- [48] K. A. Forbes and D. L. Andrews, *Phys. Rev. A* **99**, 023837 (2019).
- [49] K. A. Forbes, *Phys. Rev. Lett.* **122**, 103201 (2019).
- [50] H. P. Latscha, U. Kazmaier, and H. A. Klein, *Organische Chemie*, 6th ed. (Springer, Berlin, 2008).
- [51] J. Gal, *Chirality* **12**, 959 (2012).
- [52] T. J. Leitereg, D. G. Guadagni, J. Harris, T. R. Mon, and R. Teranishi, *J. Agric. Food Chem.* **19**(4), 785 (1971).
- [53] J. Hyttel, K. Bøgesø, J. Perrgaard, and C. Sánchez, *J. Neural Transm.* **88**(2), 157 (1992).
- [54] A. J. Hutt and S. C. Tan, *Drugs* **52**, 1 (1996).
- [55] E. J. Ariens, *Eur. J. Clin. Pharmacol.* **26**, 663 (1984).
- [56] T. Eriksson, S. Bjorkman, and P. Hoglund, *Eur. J. Clin. Pharmacol.* **57**, 365 (2001).
- [57] S. K. Teo, W. A. Colburn, W. G. Tracewell, K. A. Kook-David, I. Stirling, M. S. Jaworsky, M. A. Scheffler, S. D. Thomas, and O. L. Laskin, *Clin. Pharmacokinet.* **43**, 311 (2004).
- [58] M. Quack, *Angew. Chem., Int. Ed. Engl.* **41**, 4618 (2002).
- [59] M. Quack, J. Stohner, and M. Willeke, *Annu. Rev. Phys. Chem.* **59**, 741 (2008).
- [60] *Comprehensive Chiroptical Spectroscopy: Instrumentation, Methodologies, and Theoretical Simulations*, edited by N. Berova, P. L. Polavarapu, K. Nakanishi, and R.W. Woody (Wiley, New York, 2012).
- [61] N. Berova and K. Nakanishi, *Circular Dichroism: Principles and Applications* (Wiley, New York, 2000).
- [62] L. A. Nafie, *Vibrational Optical Activity: Principles and Applications* (Wiley, Chichester, 2011).
- [63] C. Ye, Q. Zhang, and Y. Li, *Phys. Rev. A* **98**, 063401 (2018).
- [64] Q. Zhang, Y.-Y. Chen, C. Ye, and Y. Li, *J. Phys. B: At. Mol. Opt. Phys.* **53**, 235103 (2020).
- [65] W. Happer, *Rev. Mod. Phys.* **44**, 169 (1972).
- [66] T. G. Walker and W. Happer, *Rev. Mod. Phys.* **69**, 0034 (1997).
- [67] A. Imamoglu, E. Knill, L. Tian, and P. Zoller, *Phys. Rev. Lett.* **91**, 017402 (2003).
- [68] A. Urvoy, Z. Vendeiro, J. Ramette, A. Adiyatullin, and V. Vuletić, *Phys. Rev. Lett.* **122**, 203202 (2019).
- [69] S. Hoekstra, J. J. Gilijamse, B. Sartakov, and N. Vanhaecke, L. Scharfenberg, *Phys. Rev. Lett.* **98**, 133001 (2007).
- [70] I. Manai, R. Horchani, H. Lignier, P. Pillet, and D. Comparat, *Phys. Rev. Lett.* **109**, 183001 (2012).
- [71] B. L. Augenbraun, J. M. Doyle, T. Zelevinsky, and I. Kozyryev, *Phys. Rev. X* **10**, 031022 (2020).
- [72] D. Mitra, N. B. Vilas, C. Hallas, L. Anderegg, B. L. Augenbraun, L. Baum, C. Miller, S. Raval, and J. M. Doyle, *Science* **369**, 1366 (2020).
- [73] I. Thanopulosa and P. Král, *J. Chem. Phys.* **119**, 5105 (2003).
- [74] F. Hund, *Z. Phys.* **43**, 805 (1927).
- [75] P. W. Anderson, *Phys. Rev.* **75**, 1450 (1949).
- [76] H. Margenau, *Phys. Rev.* **76**, 1423 (1949).
- [77] M. Simonius, *Phys. Rev. Lett.* **40**, 980 (1978).
- [78] M. Cattani, *J. Quant. Spectrosc. Radiat. Transfer* **46**, 507 (1991).
- [79] A. Vardi, *J. Chem. Phys.* **112**, 8743 (2000).
- [80] G. Jona-Lasinio, C. Presilla, and C. Toninelli, *Phys. Rev. Lett.* **88**, 123001 (2002).
- [81] M. Cattani and J. M. F. Bassalo, *J. Quant. Spectrosc. Radiat. Transfer* **102**, 441 (2006).
- [82] J. Trost and K. Hornberger, *Phys. Rev. Lett.* **103**, 023202 (2009).
- [83] I. Gonzalo and P. Bargaño, *Phys. Chem. Chem. Phys.* **13**, 17130 (2011).
- [84] F. T. Ghahramani and A. Shafie, *Phys. Rev. A* **88**, 032504 (2013).
- [85] C. Presilla and G. Jona-Lasinio, *Phys. Rev. A* **91**, 022709 (2015).
- [86] C. Ye, Q. Zhang, and Y. Li, *Phys. Rev. A* **99**, 062703 (2019).
- [87] H. Fröhlich, *Phys. Rev.* **79**, 845 (1950).
- [88] S. Nakajima, *Adv. Phys.* **4**, 363 (1955).
- [89] J. Hauss, A. Fedorov, C. Hutter, A. Shnirman, and G. Schön, *Phys. Rev. Lett.* **100**, 037003 (2008).
- [90] D. Patterson and J. M. Doyle, *Mol. Phys.* **110**, 1757 (2012).
- [91] T. A. Isaev and R. Berger, *Phys. Rev. Lett.* **116**, 063006 (2016).